Journal of Sound and Vibration (2001) **245**(5), 801–814
doi:10.1006/jsvi.2000.3605, available online at http://www.idealibrary.com on IDEAL®

MODELLING OF DYNAMIC RESPONSES OF AN AUTOMOTIVE FUEL RAIL SYSTEM, PART I: INJECTOR

Q. Hu and S. F. Wu

Department of Mechanical Engineering, Wayne State University, Detroit, MI 48202, *U.S.A.*

AND

S. Stottler and R. Raghupathi

Robert Bosch Corporation, 38000 *Hills Tech Drive, Farmington Hills, MI* 48331-3417, *U.S.A.*

(*Received* 1 *June* 1999, *and in final form* 22 *December* 2000)

This paper presents a computer model for simulating dynamic responses of an automotive fuel rail system. Part I of this paper deals with the mathematical modelling of an individual injector. To reduce the complexity of this problem, the injector is discretized into three segments with a filter at the top, a coil spring and needle assembly in the middle, and four orifices at the bottom. The fluid flowing through these segments is coupled and described by a one-dimensional unsteady Bernoulli's equation. Loss factors K_F and K_O are used to account for the losses of kinetic energy as fluid enters the injector through the filter at the top and discharges through orifices at the bottom respectively. The value of K_F is assumed constant and determined experimentally. The value of K_O, however, varies because the fluid kinetic energy changes with the passage cross-sectional area between the needle and the valve seat. In this investigation, K_O is correlated to the needle motion, which is governed by a second order ordinary differential equation. The forces exerted on the needle include the magnetic and coil spring forces, which control the opening and closing of the injector. The pressure fluctuations inside the injector caused by the opening and closing of the needle are described by a damped wave equation. The dynamic responses of the injector are then obtained by solving a set of nine equations simultaneously. The calculated pressure fluctuations inside an injector are compared with the measured data under various pulse widths and speeds. Good agreement is obtained in each case.

1. INTRODUCTION

The ability to control the quantity and timing of fuel delivered by an electronic fuel injection system has provided automotive engineers with a means to improve the performance and efficiency of present-day automobiles. However, as demands on fuel economy, emissions, and vehicle performance increase, more improvements on the electronic fuel injection system are being pursued. The vibrations of a fuel injection system caused by periodic opening and closing of injectors have long been identified as one of the most important noise sources of an automobile [1]. Test data have shown that these vibrations may lead to metering errors, pulse-to-pulse variations, and deterioration in the quality of spray atomization. In some cases, they may even produce resonance, which contributes to or results in fuel injection systems failure and engine damage.

An essential component in the fuel injection systems is the fuel injector. In the past decade, interesting improvements in injector designs have been proposed [2, 3]. Recently,

0022-460X/01/350801 + 14 $35.00/0

much effort has been devoted to studies of the flow inside an injector and to development of computer models to predict the dynamic responses of an injection system. For example, Becchi [4], Goyal [5], Kumar *et al.* [6], Sobel *et al.* [7], Krepec *et al.* [8], and Ziejewski *et al.* [9] used numerical techniques to simulate the pump–line–nozzle injection systems for diesel engines.

Strunk [10] showed how the design variables may influence the performance of a pump–line–nozzle injection system and provided guidelines for its tuning. These results were based on a simplified mathematical model for the hydraulic circuit of the systems. Many assumptions were made in this mathematical modelling, for example, a constant velocity of the pump piston during the injection cycle, linear resistance of the injection nozzle, negligence of the dynamics of the injector needle, etc.

Catania *et al.* [11] demonstrated simulations of a distributor-type diesel fuel injection system by using a second order ordinary differential equation for describing the injector needle motion, and a conventional lumped mass model for the continuity and compressibility of the fuel flow. Smith and Spinweber [12] constructed a digital simulation model for the solenoid fuel injector, which was divided into three sub-models for electromagnetic, mechanical, and flow field, respectively. The electromagnetic sub-model described the interaction of the iron magnetic flux path with the solenoid coil windings. The mechanical sub-model described force interaction on the injector pintle and its consequent trajectory. The flow sub-model described essentially the static flow of the injector from zero lift to full lift. Yang *et al.* [13, 14] studied dynamic responses of a multi-port electronic fuel delivery system. In their model, a third order equation was employed to account for the effects of magnetic- and flow-induced forces as well as the mechanical friction force inside the injector chamber. Spurk *et al.* [15] developed a mathematical model for BOSCH injectors in which the unsteady compressible flow inside the injector and steady incompressible flow in inlet and outlet sections were considered. The equations of motion for needle and body were derived. Some empirical parameters such as the stiffness coefficients and the damping coefficient related to the roughness between the body seat surface and the needle seat surface, and the loss coefficient for the sieve were assumed in the computation. In this way, the needle motion inside the injector and the pressure history at the valve seat were calculated.

Ren and Nally [16] utilized the axisymmetry property to model a quarter of a fuel injector from the upstream of the valve seat to the downstream of the orifice by using a non-uniform body-fit grid with a total of 105 000 computational cells. The fluid dynamics was analyzed by solving the ensemble-averaged, three-dimensional mass and momentum conservation equations. In this model, the flow was assumed to be isothermal and incompressible. The main numerical results included the relationship between the static flow rate and the fuel pressure, the relationship between the static flow rate and the orifice size, the relationship between needle lift and the discharge coefficient, and the transient effects during the opening and closing periods.

Although different models have been developed to describe the fuel injection systems, few can accurately predict the transient responses of a fuel injection system, especially the pressure fluctuations inside the injectors caused by rapid opening and closing of the valves. The present paper attempts to fill this void by developing a mathematical model to describe pressure fluctuations inside an injector. The results thus obtained are validated experimentally on a fuel rail system mounted on a test bench operating under the same conditions as those of a vehicle.

2. MODELLING OF AN INJECTOR

The fuel injector is a complex structure containing many intricate components. The major component is a solenoid actuated needle valve assembly that controls the flow

passage through the orifices at the bottom of the valve seat. Since the upstream pressure of an injector is high (3·6 bar) and the downstream pressure is low (equal to the manifold pressure inside a cylinder chamber), the needle is pushed firmly against the valve seat. When the solenoid is activated by an electrical signal from the engine controller, a magnetic force is generated that overcomes the spring force and pushes the needle upwards. As the needle is lifted, fuel accelerates from a near-zero velocity to a maximum value and discharges into the cylinder chamber through the orifices. Meanwhile, the pressure inside the injector drops to the minimum then bounces back to a maximum value. These pressure fluctuations continue, but their amplitudes decay gradually to the ambient level and remain constant until the solenoid is deactivated. Once the magnetic force is removed, the coil spring pushes the needle back to its seat and stops the flow almost instantly. This sudden blockage of the flow generates a pressure surge and fluctuations thereafter. These pressure fluctuations propagate throughout the entire fuel rail, causing the system to vibrate.

To describe the pressure fluctuations inside an injector exactly, it would be necessary to solve the entire flow field and its interaction with various boundary surfaces. Such a task is not possible even with the most advanced computer system now available. On the other hand, most engineering models oversimplify the problem and yield little insight. While some models give good correlation between the calculated and measured responses, they are often case-dependent.

In the present investigation, a mathematical model is developed that relates the responses of an injector to its design parameters. To simplify the complexity of the problem, the injector is divided into three segments with a filter at the top, a solenoid actuated needle and coil spring assembly in the middle, and four orifices at the bottom sections respectively (see Figure 1).

Assume that the fluid is homogeneous and incompressible and that the flow through each segment of an injector is unsteady but one-dimensional. Note that the fluid

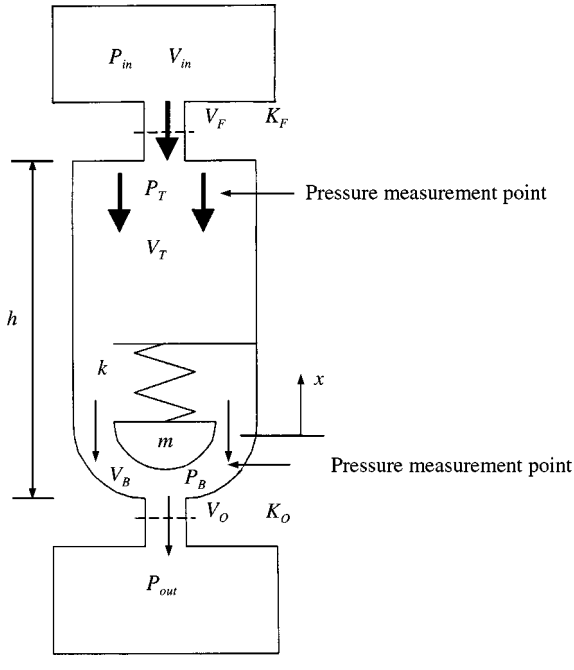

Figure 1. Schematic of test set-up for injector and pressure transducers.

incompressibility assumption is permissible because the density of the test fluid is high, the overall dimensions of the fuel rail system are small, and the upstream pressure is high (3·6 bar). The dimensions of the injector and fuel rail further allow to neglect the potential differences between any two points along the fuel rail system. Under these conditions, one can apply Newton's second law to fluid particles and integrate the equation of motion along a streamline to obtain [17]

$$P_1 + \frac{1}{2}\rho V_1^2 = P_2 + \frac{1}{2}\rho V_2^2 + \frac{\rho}{A_{av}}\frac{\mathrm{d}Q}{\mathrm{d}t}(s_2 - s_1), \tag{1}$$

where P_i and V_i represent the pressure and flow velocity at any two locations along the streamline s_i, $i = 1$ and 2, respectively, Q is the volume flow between s_1 and s_2, A_{av} is the corresponding average cross-sectional area inside an injector, and ρ is the density of the fluid.

Equations similar to equation (1) but with consideration of the loss of kinetic energy are often used to simulate the phenomena due to sudden valve closure and water hammer in pipes [18]. Introducing loss factors to account for the losses of kinetic energy as the fuel flows through the filter and orifices, we can write equations governing pressures and flow velocities at the top, middle, and bottom sections as

$$P_{in} + \tfrac{1}{2}\rho V_{in}^2 = P_T + \tfrac{1}{2}\rho V_T^2 + \tfrac{1}{2}\rho K_F V_F^2, \tag{2a}$$

$$P_T + \frac{1}{2}\rho V_T^2 = P_B + \frac{1}{2}\rho V_B^2 + \frac{\rho h}{A_{av}}\frac{\mathrm{d}Q}{\mathrm{d}t}, \tag{2b}$$

$$P_B + \frac{1}{2}\rho V_B^2 + \rho h\frac{\mathrm{d}V_{av}}{\mathrm{d}t} = P_{out} + \frac{1}{2}\rho K_O V_O^2, \tag{2c}$$

where P_{in} and P_{out} are the pressure at the inlet and outlet of the injector, respectively, V_{in} and V_O are the corresponding flow velocities at these two locations, P_T and P_B are the pressures at the top and bottom sections inside the injector, respectively, V_T and V_B are the corresponding flow velocities, V_F is the flow velocity passing through the filter, and $h = (s_T - s_B)$ is the length of the injector.

Note that in this case the inlet and outlet are immediately adjacent to the top and bottom sections of the injector, $(s_{in} - s_T) \to 0$ and $(s_B - s_O) \to 0$. Hence the last term on the right-hand side of equation (1) is omitted in equations (2a) and (2c). Further, we assume that loss of kinetic energy occurs only at the top and bottom of an injector. Therefore, loss factors K_F and K_O are introduced in equations (2a) and (2c), which describe the losses of kinetic energy as the fluid enters the injector through the filter at the top and as the fluid is discharged through orifices at the bottom sections respectively.

Applying the mass conservation law [19] to the top and bottom sections of the injector yields, respectively, leads to

$$V_{in}A_{in} = V_T A_T, \qquad Q = V_B A_B = V_O A_O, \tag{3a, b}$$

where A_{in}, A_T, A_B and A_O are the cross-sectional areas of fuel passage through the inlet, top section, bottom section, and orifices of the injector respectively.

Since the filter is fixed, it is reasonable to assume a constant value for the loss factor K_F, which can be determined experimentally. Applying the mass conservation law between the inlet and the top section of the injector, we have

$$Q_F = V_{in}A_{in} = V_F A_F = V_T A_T, \tag{4}$$

TABLE 1

Parameters used in simulating the magnetic force f_m

n	b_n	ω_n
1	0·9620	714
2	− 0·1739	2142
3	− 0·1264	3570
4	0·0582	4998
5	0·0264	6426
6	− 0·0265	7854
7	− 0·0240	9282

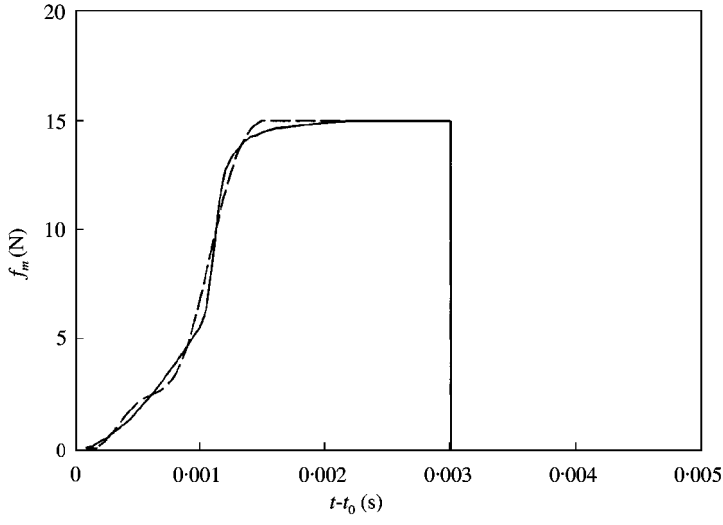

Figure 2. Simulation of the magnetic force acting on the needle: ——, measured; – – –, simulated.

where Q_F is the volume flow passing through the filter and A_F the cross-sectional area of the filter. Using equations (2a) and (4), we can then write K_F as

$$K_F = \frac{2(P_{in} - P_T)A_F^2}{\rho Q_F^2} + A_F^2\left(\frac{1}{A_{in}^2} - \frac{1}{A_T^2}\right). \tag{5}$$

Therefore, by measuring the flow into the injector, the pressure difference $(P_{in} - P_T)$ across the filter, and the cross-sectional areas A_F, A_{in}, and A_T, we can determine K_F.

The loss factor K_O can be estimated using the theory of internal flows through a sudden expansion chamber [20]. In this particular case the expansion occurs around the valve seat. Moreover, the loss of the fluid kinetic energy changes with the passage cross-sectional area between the needle and the valve seat, which varies with the needle motion. Consequently, K_O is defined as a function of the needle displacement x, which is governed by a second

order ordinary differential equation.

$$K_O = 1 + \left(\frac{A_O}{xD}\right)^2 \begin{cases} \left(1 - \dfrac{xD}{A_B}\right)^2, & x \leqslant \dfrac{A_B}{D}, \\ \left(1 - \dfrac{A_B}{xD}\right)^2, & x > \dfrac{A_B}{D}, \end{cases} \tag{6}$$

where D is the diameter of the bottom section inside the injector and x satisfies the equation of motion

$$m\ddot{x} + c_0\dot{x} + kx = -f_p + f_m, \tag{7}$$

where m represents the lumped mass of the needle, k stands for the spring constant, c_0 is the viscous damping coefficient of the spring, and f_p and f_m are the spring pre-loading and magnetic forces exerted on the needle respectively. Note that because of a small cross-sectional area ($<10^{-6}\,\mathrm{m}^2$), the effect of the fluid force on the needle is negligibly small. Numerical results demonstrate that omission of the fluid force has little impact on the responses of needle motion.

Test data show that when the solenoid is activated, the magnitude of the magnetic force f_m rises from zero to maximum in a non-linear manner. Experimental results indicate that the time it takes for the magnetic force to reach its maximum value is approximately 1·5 ms. However, when the solenoid is deactivated, the magnitude of f_m drops to zero instantly. Based on the measured data, an empirical formula is developed to describe the rise and fall of this magnetic force f_m.

$$f_m(t) = f_{max}\lfloor H(t - t_0) - H(t - t_0 - t_p)\rfloor \times \left[H(t_0 + 0{\cdot}0015 - t) \sum_{n=1}^{7} b_n \sin \omega_n (t - t_0) + H(t - t_0 - 0{\cdot}0015) \right], \tag{8}$$

where f_{max} is the maximum value of the magnetic force, t_0 the time when the solenoid is activated, and t_p the pulse width during which the magnetic force is sustained. The values of b_n and ω_n, $n = 1$–7, are given in Table 1. Figure 2 shows the comparison of measured and simulated magnetic forces using equation (8) as the solenoid is activated and deactivated. Note that t_0 is periodic synchronizing with the engine speed and t_p is fixed for a particular engine design.

The pressure fluctuations caused by opening and closing of the needle will propagate throughout the entire fuel rail system. To describe this propagation phenomenon, we require the pressure fluctuations to satisfy the wave equation, which can be derived by applying the Navier–Stokes equation to a one-dimensional laminar flow of a Newtonian fluid [21], using the continuity [22] and thermodynamic [23] equations, and neglecting the high order terms:

$$\frac{\partial^2 P}{\partial y^2} - \frac{1}{c^2}\frac{\partial^2 P}{\partial t^2} = -\frac{v}{c^2}\frac{\partial^3 P}{\partial t \partial y^2}, \tag{9}$$

where y is the co-ordinate in the flow direction inside the injector, t the time, c the speed of sound of the fluid, and v the kinematic viscosity. The pressure fluctuations are related to velocities by the following linearized moment equation:

$$\frac{\partial V}{\partial y} = -\frac{1}{\rho c^2}\frac{\partial P}{\partial t}. \tag{10}$$

TABLE 2

Input of typical injector design parameters and material properties of test fluid

Parameters	Descriptions
m	Mass of the needle
k	Coil spring constant acting on the needle
c_0†	Approximate damping coefficient acting on the needle
f_p	Pre-loading coil spring force acting on the needle
f_{max}	Maximum magnetic force acting on the needle
K_F	Loss factor for the filter at the top
h	Length of the injector
D	Diameter of the bottom section
A_{in}	Cross-sectional area at the inlet
A_F	Cross-sectional area of the filter
A_T	Cross-sectional area of the top section
A_B	Cross-sectional area of the bottom section
A_O	Cross-sectional area of all orifices
A_{av}	Average cross-sectional area of the injector
ρ	Density of n-heptane
c	Approximate speed of sound of n-heptane
v	Approximate viscosity of n-heptane

† Note that in this paper $c_0 = 1$ (N s/m) is selected for the sake of convenience. The exact value of the damping coefficient of the coil spring is unknown. However, numerical tests indicate that the pressure fluctuations are not sensitive to the value of c_0.

Equations (2)–(10) completely define the pressure fluctuation responses inside a fuel injector.

3. TEST SET-UP

The mathematical model described above is validated experimentally. To measure the responses of an injector, two Kulite XT-123C-100 pressure transducers were installed, one at the top (near the entrance) and the other at the bottom (above the orifices) sections (see Figure 1). This instrumented injector was mounted on a fuel rail system consisting of a fuel tank, pump, regulator, controller, supply and return lines. A pressure regulator was used to maintain a constant back pressure, and a controller was used to control the opening and closing of the injector. With this set-up, one can simulate various working conditions of a fuel injection system under different injector pulse widths and engine speeds. In this investigation, the pressure fluctuations were measured under three different speeds, namely, 700, 750, and 1050 r.p.m. respectively. These speeds were chosen to simulate engine idle and off-idle conditions. For each of these speeds, the pulse widths were set at 2·5 and 7 ms respectively. The fluid used in the experiments was *n*-heptane, which has the same viscosity and density as those of gasoline, but provides greater stability. The measured data were recorded and stored in a desktop computer automatically for post-processing. The sampling rate of data acquisition was set at 24 kHz.

4. VALIDATIONS

The responses of an injector were obtained by solving equations (2)–(10) simultaneously. In particular, the wave equation (9) was solved by using finite (backward) difference method [21]. The pressure boundary conditions at the inlet and outlet were P_{in} and P_{out} respectively.

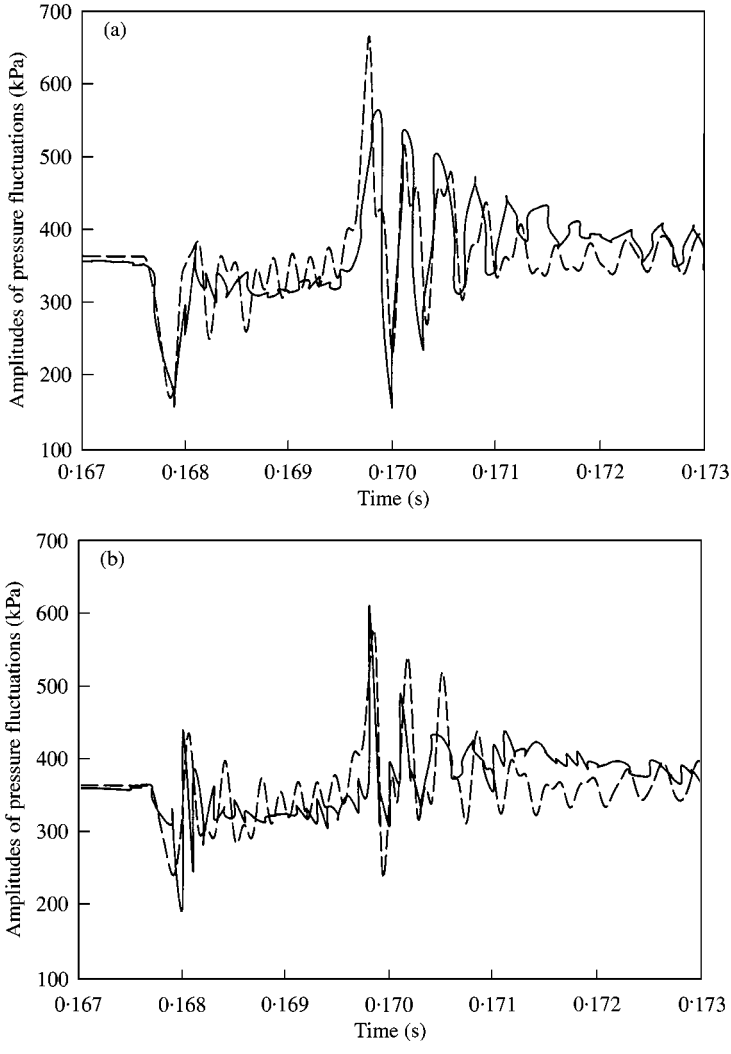

Figure 3. Comparison of pressure fluctuations inside an injector at 700 r.p.m. and 2·5 ms pulse width: (a) bottom; (b) top; ——, measured; – – –, calculated.

Note that the flow passages inside an injector were not straight, but had twists and turns. Since an accurate trace of flow passage was not possible, the exact length of flow passage inside an injector was unknown. Numerical tests indicated that satisfactory results could be obtained when the length of flow passage was set at four times the injector length h. This effective flow passage was discretized into nine segments and the pressure fluctuations at all nodes along this passage were calculated. The values of pressure fluctuations corresponding to the locations of P_T and P_B were then compared with the measured data.

In carrying out the numerical computations, dimensions of an injector must be specified. Table 2 lists some typical design parameters and properties of the test fluid as the input to the computer model.

Substituting the parameters given in Table 2 into equations (2)–(10), we can solve pressure fluctuations at various locations inside the injector. Figure 3 demonstrates

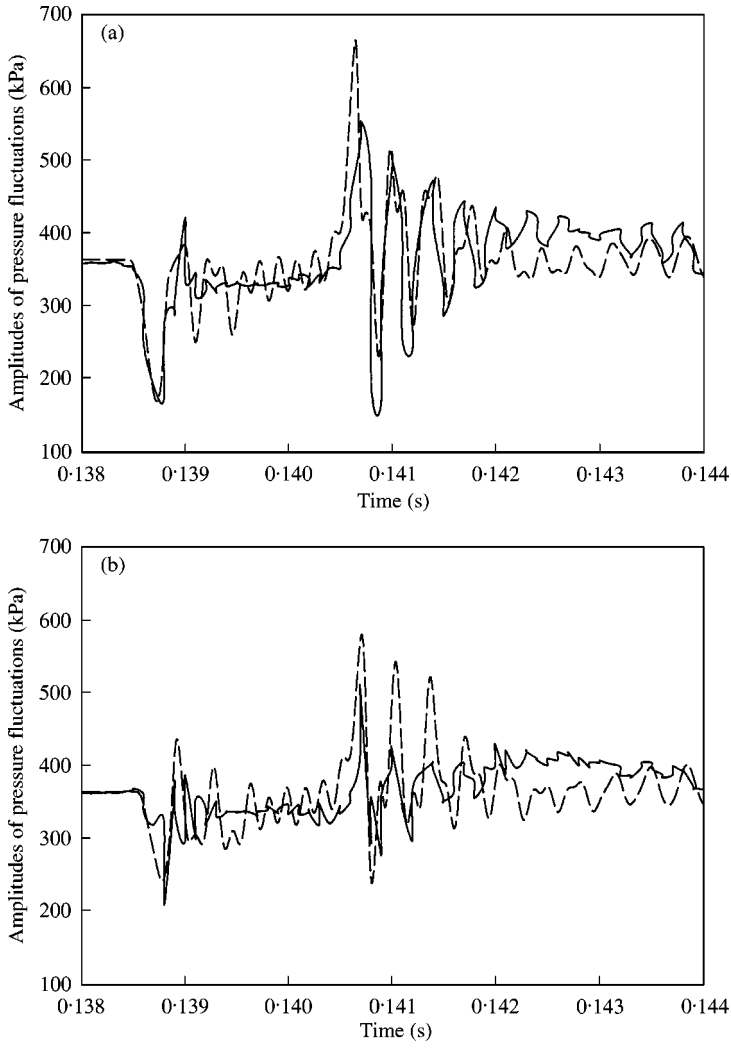

Figure 4. Comparison of pressure fluctuations inside an injector at 750 r.p.m. and 2·5 ms pulse width: (a) bottom; (b) top; ——, measured; – – –, calculated.

comparisons of the calculated and measured pressure fluctuations at the bottom and top sections of the injector at 700 r.p.m. and a 2·5 ms pulse width.

Results show that the present computer model is capable of capturing the main characteristics of pressure fluctuations inside an injector. As the injector is opened, the pressure drops immediately because of rarefaction. This rarefaction is followed by rapid oscillations that decay exponentially to the ambient level due to fluid viscosity. When the injector is closed suddenly, compression occurs, which causes a strong pressure surge known as the "water hammer" effect inside the injector. The amplitude of this pressure surge decays exponentially in an oscillatory manner to the ambient level as the injector remains closed. These pressure drops and surges inside an injector and fuel rails are periodic, synchronizing with the engine's cyclic motion. In this paper, we only display comparisons of pressure fluctuations around the opening and closing of an injector (about 6–10 ms) in order

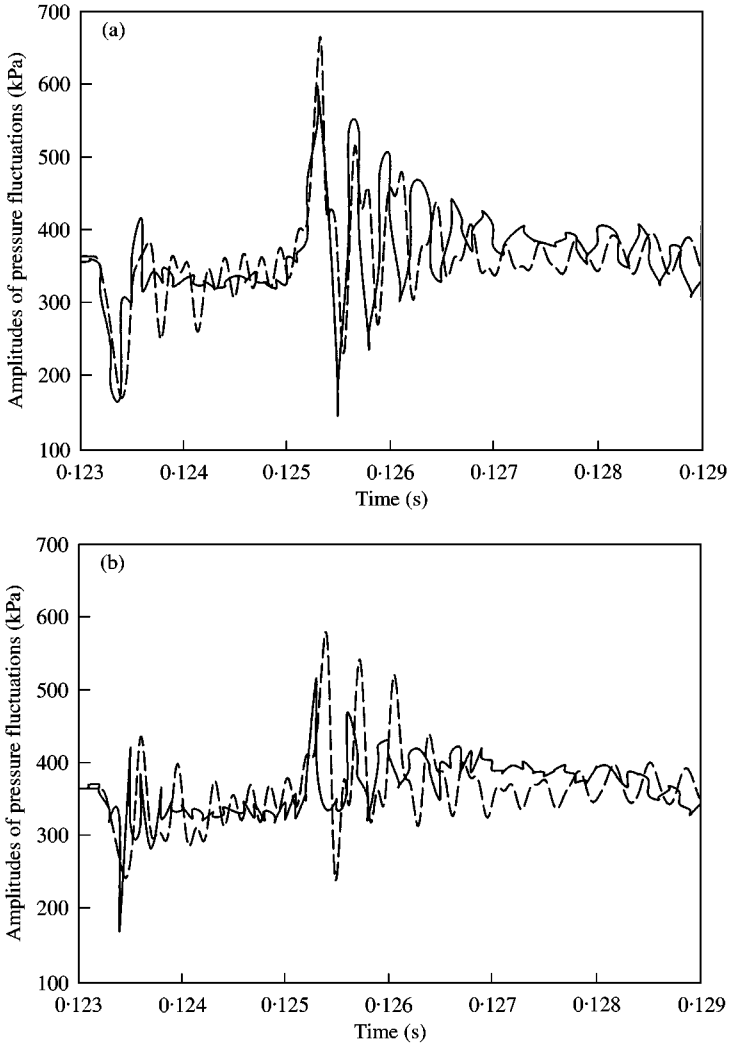

Figure 5. Comparison of pressure fluctuations inside an injector at 1050 r.p.m. and 2·5 ms pulse width: (a) bottom; (b) top; ——, measured; – – –, calculated.

to show the details of oscillations. If comparisons were given for an entire cycle, which is about 57·1–85·7 ms for 700–1050 r.p.m., the plots would consist of pockets of overcrowded peaks at the opening and closing times and nothing in between, which would make validations of the present computer model difficult.

Experimental data indicate that the amplitude of the pressure surge or drop can be twice as high (or low) as that of the ambient level. These pressure surges and drops are the major sources of vibration, noise, and metering errors of a fuel injection system.

Figure 3 shows that the calculated pressure drop at the bottom section as the injector is just opened agrees almost perfectly with the measured data. The calculated pressure surge at the same location when the injector is suddenly closed is overestimated by 30 per cent. This discrepancy may be due to a rigid boundary condition at the seat in the modelling, which leads to a higher value of pressure surge than the actual one. However,

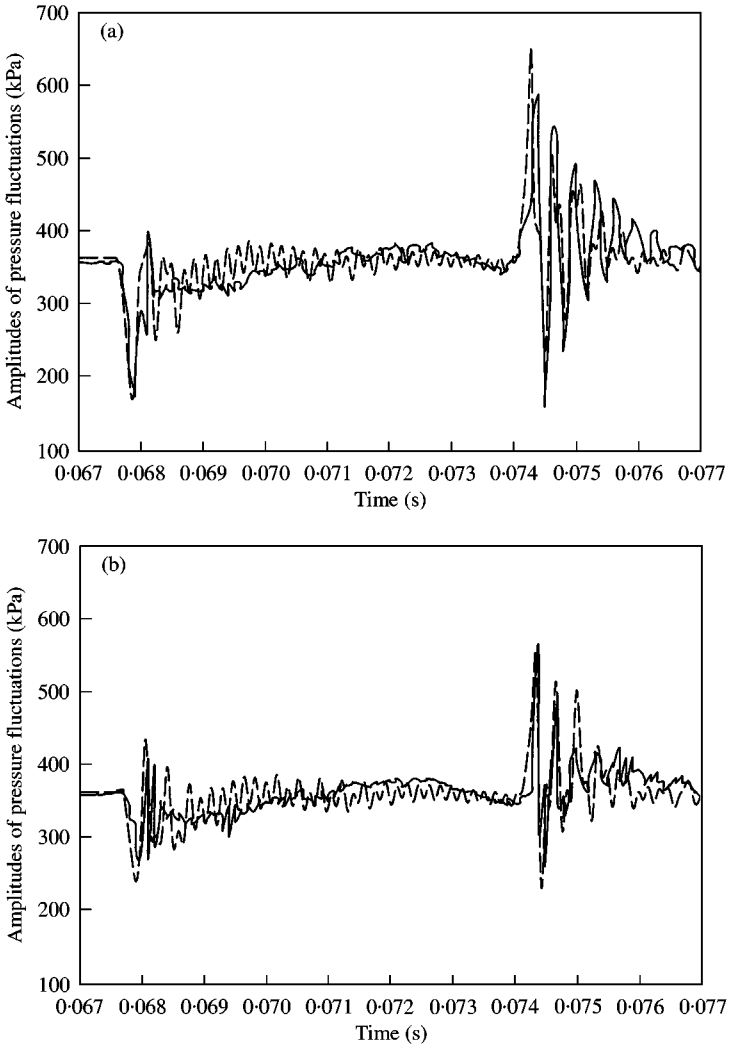

Figure 6. Comparison of pressure fluctuations inside an injector at 700 r.p.m. and 7 ms pulse width: (a) bottom; (b) top; ——, measured; – – –, calculated.

the decay of pressure fluctuations after the pressure surge agrees well with the measured data (see Figure 3(a)). The calculated pressure drop and surge at the top section when the injector is opened and closed agree satisfactorily with the measured data. However, the decays of the calculated pressure fluctuations at the top section after the injector is opened and closed are slower than the measured ones (see Figure 3(b)). These discrepancies could be attributed to the deterioration of the pressure transducers' performance in the high-frequency regime. In other words, the transducer may fail to respond to the high-frequency fluctuations consistently. Also, the sampling rate of 24 kHz may not be high enough, thus resulting in a relatively flat pressure fluctuation curve rather than an oscillatory one.

Similar phenomena are observed in other situations. Figures 4 and 5 depict comparisons of the pressure fluctuations under the same pulse width but at 750 and 1050 r.p.m.

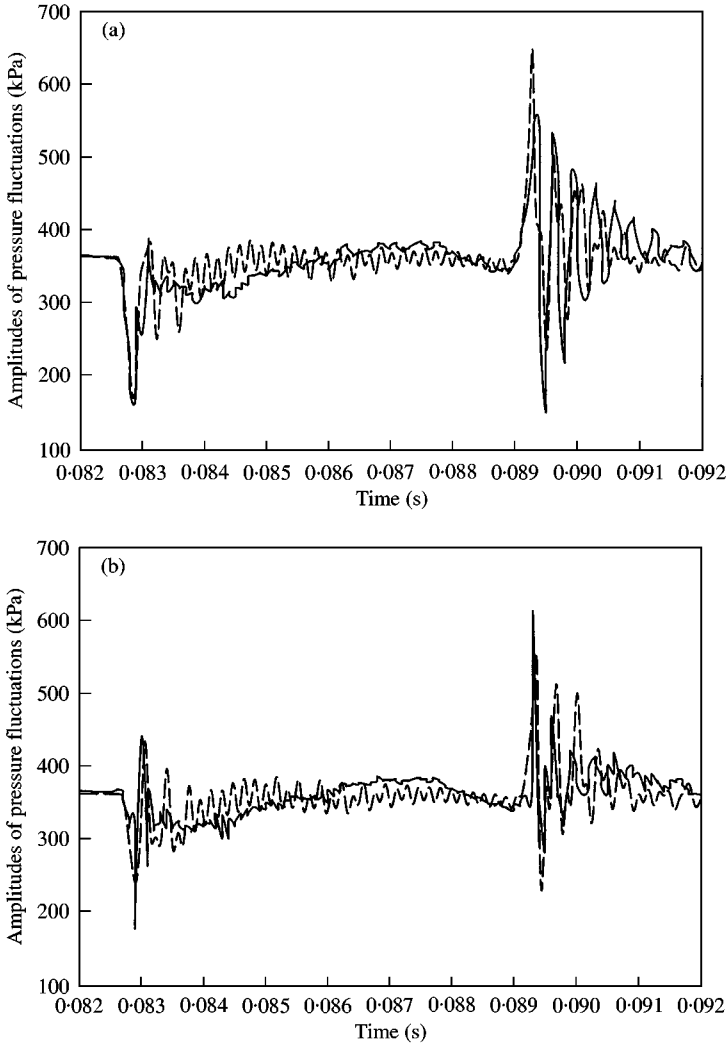

Figure 7. Comparison of pressure fluctuations inside an injector at 750 r.p.m. and 7 ms pulse width: (a) bottom; (b) top; ——, measured; – – –, calculated.

respectively. Comparisons of the calculated and measured fluctuations at these same locations but at 7 ms pulse width and three different speeds are illustrated in Figures 6–8 respectively.

5. CONCLUDING REMARKS

A computer model is developed for predicting dynamic responses of an automotive fuel injector. The pressures inside an injector are described by one-dimensional unsteady Bernoulli's equations. The fluid kinetic energy at orifices is correlated to needle motion, which is controlled by the magnetic and pre-loading coil spring forces. Further, the pressure fluctuations are required to satisfy a damped wave equation. The computer model thus developed captures the main characteristics of the responses of an injector. The calculated pressure fluctuations agree with the measured data under various working conditions in

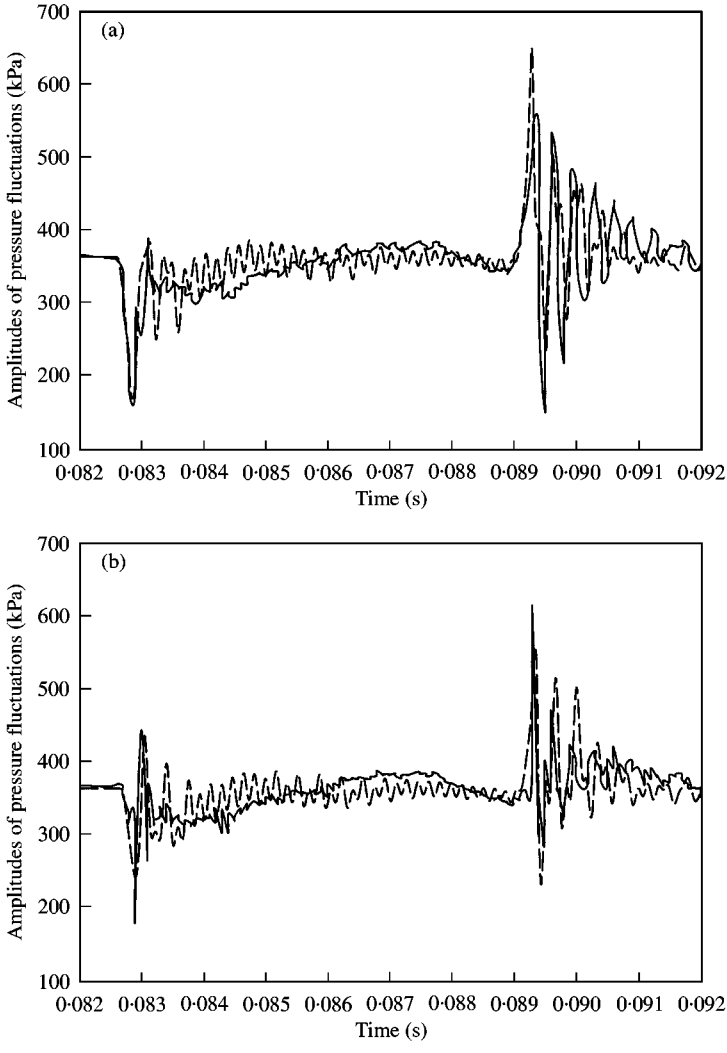

Figure 8. Comparison of pressure fluctuations inside an injector at 1050 r.p.m. and 7 ms pulse width: (a) bottom; (b) top; ——, measured; – – –, calculated.

general. Some discrepancies around pressure surge are observed. One reason could be the deterioration of the pressure transducers' performance in the high-frequency regime and the low sampling rate of experimental data.

ACKNOWLEDGMENTS

The authors wish to thank Mr Rick Wolski, Mr Keoin Grabowski, and Mr Ralf Vollmer for assisting with the collection of experimental data in this project. This work was sponsored by the Robert Bosch Corporation.

REFERENCES

1. U. Seiffert and P. Waalzer 1984 *The Future for Automotive Technology*, 34–41. London: Frances Printer (Publishers), and NH: Dover.

2. L. G. DeGrace and G. T. Bata 1985 *SAE Paper* 850559. Bendix DEKA fuel injector series—design and performance.
3. M. Greine, P. Romann and U. Steinbrenner 1987 *SAE Paper* 870124. BOSCH fuel injector—new developments.
4. G. H. Becchi 1971 *SAE Paper* 710568. Analytical simulation of fuel injection in diesel engines.
5. M. Goyal 1978 *SAE Paper* 780162. Modular approach to fuel injection system simulation.
6. D. Kumar, R. Gaur and M. G. Babu 1983 *SAE Paper* 831337. A finite-difference scheme for the simulation of a fuel injection system.
7. D. R. Sobel and R. P. C. Lehrach 1987 *SAE Paper* 870432. A hydro-mechanical simulation of diesel fuel injection systems.
8. T. Krepec and C. H. To 1988 *SAE Paper* 881855. Optimization of diesel injectors using computer aided technique.
9. M. Ziejewski and H. J. Goetter 1989 *SAE Paper* 890448. Discharge coefficients for multi-hole fuel injection nozzle for alternate fuels.
10. R. D. Strunk 1991 *SAE Paper* 911818. The dynamics of pump–line–nozzle fuel injection systems.
11. A. E. Catania, C. Dongiovanni, A. Mittica, M. Badami and F. Lovisolo 1994 *Transactions of the American Society of Mechanical Engineers Journal of Engineering for Gas Turbines and Power* **116**, 814–830. Numerical analysis versus experimental investigation of a distributor-type diesel fuel-injection system.
12. D. H. Smith and D. A. Spinweber 1980 *SAE Paper* 800508. A general model for solenoid fuel injector dynamics.
13. W. C. Yang, J. M. Glidewell, W. E. Tobler and G. K. Chui 1991 *Transactions of the American Society of Mechanical Engineers Journal of Dynamic Systems, Measurement, and Control* **113**, 143–151. Dynamic modeling and analysis of automotive multi-port electronic fuel delivery system.
14. W. C. Yang and W. E. Tobler 1991 *Transactions of the American Society of Mechanical Engineers Journal of Dynamic Systems, Measurement, and Control* **113**, 152–162. Dissipative model approximation of fuel transmission line using linear friction model.
15. J. H. Spurk, T. Betzel and N. Simon 1992 *SAE Paper* 920621. Interaction of nonlinear dynamics and unsteady flow in fuel injectors.
16. W. Ren and J. F. Nally Jr. 1996 *Proceedings of the American Society of Mechanical Engineers Fluids Engineering Division* **242**, 141–147. Computer modeling of steady and transient flows within a gasoline fuel injector.
17. Richard H. F. Pao 1965 *Fluid Mechanics*. New York: John Wiley and Sons, Inc.
18. D. R. L. Smith 1960 *Fluid Mechanics through Worked Examples*. Cleaver-Hume Press.
19. Robert L. Mott 1994 *Applied Fluid Mechanics*. New York: Maxwell Macmillan International.
20. D. S. Miller 1990 *Internal Flow Systems*. Cranfield, Bedford, UK: BHRA Information Services; second edition.
21. M. B. Abbott and D. R. Basco 1989 *Computational Fluid Dynamics*: *an Introduction for Engineers*. Harlow, Essex, England: Longman Scientific & Technical.
22. G. J. Sharpe 1994 *Solving Problems in Fluid Dynamics*. Harlow, England. Longman Scientific & Technical.
23. Malcolm. J. Crocker 1998 *Handbook of Acoustics*. New York: John Wiley & Sons, Inc.